ChemInform Abstract: Three New Cembranoid-Type Diterpenes from Red Sea Soft Coral Sarcophyton glaucum: Isolation and Antiproliferative Activity Against HepG2 Cells.

ARTICLE *in* CHEMINFORM · DECEMBER 2014

Impact Factor: 0.74 · DOI: 10.1016/j.ejmech.2014.05.016

European Journal of Medicinal Chemistry 81 (2014) 314–322

Contents lists available at ScienceDirect

European Journal of Medicinal Chemistry

journal homepage: http://www.elsevier.com/locate/ejmech

Original article

Three new cembranoid-type diterpenes from Red Sea soft coral *Sarcophyton glaucum*: Isolation and antiproliferative activity against HepG2 cells

Sultan S. Al-Lihaibi [a], Walied M. Alarif [a], Ahmed Abdel-Lateff [b,c,*], Seif-Eldin N. Ayyad [d], Ashraf B. Abdel-Naim [e], Fardous F. El-Senduny [f], Farid A. Badria [g]

[a] Department of Marine Chemistry, Faculty of Marine Sciences, King Abdulaziz University, P.O. Box 80207, Jeddah 21589, Saudi Arabia
[b] Department of Natural Products and Alternative Medicine, Faculty of Pharmacy, King Abdulaziz University, P.O. Box 80260, Jeddah 21589, Saudi Arabia
[c] Department of Pharmacognosy, Faculty of Pharmacy, Minia University, Minia 61519, Egypt
[d] Department of Chemistry, Faculty of Science, King Abdulaziz University, P.O. Box 80203, Jeddah 21589, Saudi Arabia
[e] Department of Pharmacology and Toxicology, Faculty of Pharmacy, King Abdulaziz University, P.O. Box 80260, Jeddah 21589, Saudi Arabia
[f] Department of Chemistry, Faculty of Science, Mansoura University, Mansoura 35516, Egypt
[g] Department of Pharmacognosy, Faculty of Pharmacy, Mansoura University, Mansoura 35516, Egypt

ARTICLE INFO

Article history:
Received 11 November 2013
Received in revised form
1 May 2014
Accepted 3 May 2014
Available online 5 May 2014

Keywords:
Sarcophyton
Cembranes
Antiproliferative
HepG2
PC-3

ABSTRACT

Three new cembranoids: sarcophytolol (**1**), sarcophytolide B (**2**), and sarcophytolide C (**3**), along with three known metabolites: 10(14)aromadendrene (**4**), deoxosarcophine (**5**), and sarcophine (**6**) were obtained from the soft bodied coral *Sarcophyton glaucum*. The structures were determined based on spectroscopic measurements (NMR, UV, IR and MS). Compounds **1**, **3**, and **4** had similar significant cytotoxic effects towards HepG2 (Human hepatocellular liver carcinoma; $IC_{50} = 20$ μM). **2** and **3** showed activity against MCF-7 (Human breast adenocarcinoma; IC_{50} 25 ± 0.0164 and 29 ± 0.030 μM, respectively). Finally, **4** showed potent activity towards PC-3 (Prostate cancer; IC_{50} 9.3 ± 0.164 μM). The antiproliferative activity of **1**, **3** and **4**, can be attributed, at least partly, to their ability to induce cellular apoptosis.

1. Introduction

The oceans cover Ca 70% of the whole earth and have nearly one million multicellular (Plants and animals) and one billion unicellular (Distributed under 100 different phyla) organisms [1,2]. Living in harsh environment makes the marine organisms struggling to survive and protect themselves, through chemical defense mechanism. Thus, marine organisms represent a generator for metabolites with diversity of chemical structures and biological activities [3]. The Red Sea represents the tropical and subtropical climatic region with variety of the endemic biota. Up-to-date ca 180 soft corals species were identified world-wide. The majority of them are native to the Red Sea [4]. Soft corals are known with the production of terpenoidal metabolites especially cembrane diterpenes and sesquiterpenes [5].

Soft corals, belonging to the genus *Sarcophyton* (Phylum Cnidaria; Order Alcyonacea; Family Alcyoniidae) contains 46 species with common name toadstool corals. It is attractive in color and shape [5]. It has a rounded trunk which firmly attached to the substrate. This genus is well recognized as a rich source of macrocyclic cembrane-type diterpenoids and biscembranoids. Up to date more than 300 natural cembranoid derivatives were isolated [6].

Cembrane-type diterpenoids are a large family with diversity of functionality and obtained from both terrestrial and marine organisms. They are usually exhibit cyclic ether, lactone, or furane moieties around the cembrane framework. The cembranoid-derivatives play an important role in the biomedical perspective [6–12]. The Antiproliferative is the most remarkable property of this class of diterpenoids. Their basic chemical structural patterns typically featured a common 14-membered carbocyclic nucleus and unconventional cembranoids containing a 12-, or 13-or 14-membered variants [11,12].

* Corresponding author. Department of Natural Products and Alternative Medicine, Faculty of Pharmacy, King Abdulaziz University, P.O. Box 80260, Jeddah 21589, Saudi Arabia.
E-mail address: ahmedabdellateff@yahoo.com (A. Abdel-Lateff).

http://dx.doi.org/10.1016/j.ejmech.2014.05.016
0223-5234/

The main objective of the current paper is the identification and evaluation of the antiproliferative principles isolated from the soft coral, particularly, *Sarcophyton glaucum*, collected from the Saudi Red Sea water. Extensive fractionation of the organic extract employing NP-Silica gel, preparative TLC and HPLC yielded three new cembranoids; sarcophytolol (**1**), sarcophytolide B (**2**) and sarcophytolide C (**3**) (Table 1; Figs. 1 and 2), along with two known ones; deoxosarcophine (**5**) and sarcophine (**6**), and a known sesquiterpene, 10(14)aromadendrene (**4**).

2. Results and discussion

2.1. Chemistry

The current results showed the isolation of three cembranoids; sarcophytolol (**1**), sarcophytolide B (**2**) and sarcophytolide C (**3**), along with two known, deoxysarcophine (**5**) and sarcophine (**6**), and known sesquiterpene, 10(14)aromadendrene (**4**), were obtained (Fig. 1).

The explanation of the biological mechanism of new cembranoids (**1**–**3**) and a known sesquiterpene (**4**) were performed. It was clear from the results that **1** and **4** showed potent Antiproliferative activities against HepG2 (IC_{50} 20 ± 0.032 and 20 ± 0.068 μM, respectively) and to PC-3 (IC_{50} 31.5 ± 0.053 and 9.3 ± 0.164 μM, respectively). Compounds **2** and **3** showed antiproliferative activity against MCF-7 (IC_{50} 25 ± 0.0164 and 29 ± 0.030 μM, respectively), while **3** showed significant activity towards HepG2 (IC_{50} 20 ± 0.153 μM) (Table 3). The metabolites which have antiproliferative effects with IC_{50} lower than 20 μM were subjected for cell cycle analyses. The antiproliferative activity of **1**, **3** and **4**, was attributed to effects G0/G1 and S-phase cell cycle arrest.

Compound **1** was isolated as colorless oil (8.0 mg) with $[\alpha]_D^{22}$ + 10.0 (*c* 0.02, $CHCl_3$). The structure elucidation commenced when the molecular formula of **1**, $C_{20}H_{34}O_2$ (four unsaturations) was established by LCESIMS (negative mode) *m/z* = 305.2 $[M - H]^+$ and 287.1 $[M - H_2O]^+$. This result was validated by HRESIMS (positive mode) *m/z* = 307.2632 $[M + H]^+$. The ^{13}C (^1H decoupled) and DEPT experiments allowed the determination of 20 resonances attributable to five methyles, six methylenes, six methines and three quaternary carbons.

Two of the four elements of unsaturation, are attributed to two C=C double bonds (Table 1), thus the molecule is bicyclic. The presence of hydroxyl function was deduced from the absorption band at υ_{max} 3423 cm^{-1} in the IR spectra. From the ^1H–^1H COESY spectrum of **1**, the coupling between H_3-16 resonating at δ_H 0.88 and H-15 at δ_H 1.18–1.20 (m), as well as this signal and the H_3-17 at δ_H 0.73 indicated the presence of isopropyl moiety. The presence of this moiety and its connection to C-1 were established by Long-range C–H correlations observed between the resonances of H_3-16 and those of C-1 (δ_C 46.6), C-15 (δ_C 29.0), and C-17 (δ_C 20.3), between H_3-17 and C-1, C-15, and C-16 (δ_C 20.8). The existence of a furan ring was concluded by studying the correlations observed between H-1 resonating at δ_H (1.32–1.34) and both H-2 at δ_H 4.53 and H-14 at δ_H 3.88, in addition to the long-range correlations between H-1 with C-2 (δ_C 71.1), C-3 (δ_C 125.4), C-13 (δ_C 75.0), C-14 (δ_C 71.9), C-15 (δ_C 29.0), C-16 (δ_C 20.8) and C-17 (δ_C 20.3). Furthermore, HMBC correlation between H-2 and C-1 (δ_C 46.6), C-2 (δ_C 71.1), C-13 (δ_C 75.0) and C-14 (δ_C 71.9); also correlation between H_3-20 (δ_H 1.02, s) and C-13 and C-14 indicated the connection between C-13 and C-14 and positioning of CH_3-20 on C-13, thus the five membered ring was closed by ether link between C-2 and C-13. On these bases the positioning of the isopropyl group to be attached to C-1 and then the furan ring was established. The presence of a furan

Table 1
^1H [$CDCl_3$, 600 MHz] and ^{13}C NMR [$CDCl_3$, 150 MHz] NMR spectral data of **1**–**3**.[a]

P.	**1**		**2**		**3**	
	δ_C[b]	δ_H[c]	δ_C	δ_H	δ_C	δ_H
1	46.6	1.33–1.34 (m)	162.2	–	162.9	–
2	71.1	4.53 (dd, 10.2, 5.4 Hz)	36.4	2.01 (ddd, 13.2, 10.8, 2.4 Hz) 2.20 (ddd, 18.0, 12.6, 9.0 Hz)	36.9	2.40 (ddd, 10.8, 4.2, 3.0 Hz)
3	125.4	5.27 (d, 10.2 Hz)	25.2	1.91–1.93 (m) 1.69–1.71 (m)	25.8	1.90–1.93 (m) 1.69–1.71 (m)
4	138.6	–	61.4	2.68 (dd, 4.8, 4.2 Hz)	61.8	2.66 (dd, 6.6, 6.0 Hz)
5	39.9	2.18–2.21 (m) 1.97–1.99 (m)	59.9	–	60.2	–
6	25.2	2.31–2.33 (m) 2.11–2.12 (m)	39.0	1.08 (ddd, 3.0, 7.0, 17.4 Hz)	38.5	1.10 (ddd, 3.0, 7.0, 17.4 Hz)
7	124.1	5.00 (dd, 10.2, 5.4 Hz)	23.3	2.13 (dd, 3.0, 7.0 Hz)	23. 0	2.18 (dd, 3.0, 7.0 Hz)
8	136.0	–	144.1	–	144.9	–
9	33.7	2.42 (t, 3.6 Hz) 2.39 (t, 3.6 Hz)	124.9	5.17 (dd, 9.6, 5.4 Hz)	124.6	5.11 (dd, 8.4, 7.8 Hz) 2.03–2.05 (m)
10	18.7	1.75–1.77 (m) 1.25–1.27 (m)	37.4	2.40 (ddd, 10.8, 4.2, 3.0 Hz)	35.1	2.18–2.21 (m)
11	31.9	1.78–1.79 (m) 1.28–1.30 (m)	27.6	2.10 (ddd, 13.2, 5.4, 2.4 Hz) 2,78 (ddd, 18.0, 9.6, 7.8 Hz)	26.8	2.05–2.08 (m) 2.69–2.71 (m)
12	35.2	2.13–2.15 (m) 1.99–2.10 (m)	135.6	–	134.5	–
13	75.0	–	122.9	5.05 (dd, 10.2, 1.2 Hz)	123.1	4.99 (dd, 9.6, 1.2 Hz)
14	71.9	3.88 (d, 9.6 Hz)	78.8	5.57 (dd, 10.2, 1.2 Hz)	79.9	5.45 (dd, 9.6, 1.2 Hz)
15	29.0	1.18–1.20 (m)	120.6	–	119.1	–
16	20.8	0.88 (d, 6.6 Hz)	174.0	–	175.0	–
17	20.3	0.73 (d, 6.6 Hz)	15.4	1.65 (s)	15.5	1.60 (s)
18	24.2	1.65 (3H, s)	17.1	1.28 (s)	18.1	1.27 (s)
19	17.3	1.61 (3H, s)	16.1	1.91 (s)	16.7	1.93 (s)
20	15.1	1.02 (3H, s)	8.92	1.88 (s)	9.2	1.86 (s)

[a] All assignments are based on 1D and 2D measurements (HMBC, HSQC, COESY).
[b] Implied multiplicities were determined by DEPT (C = s, CH = d, CH_2 = t).
[c] *J* in Hz.

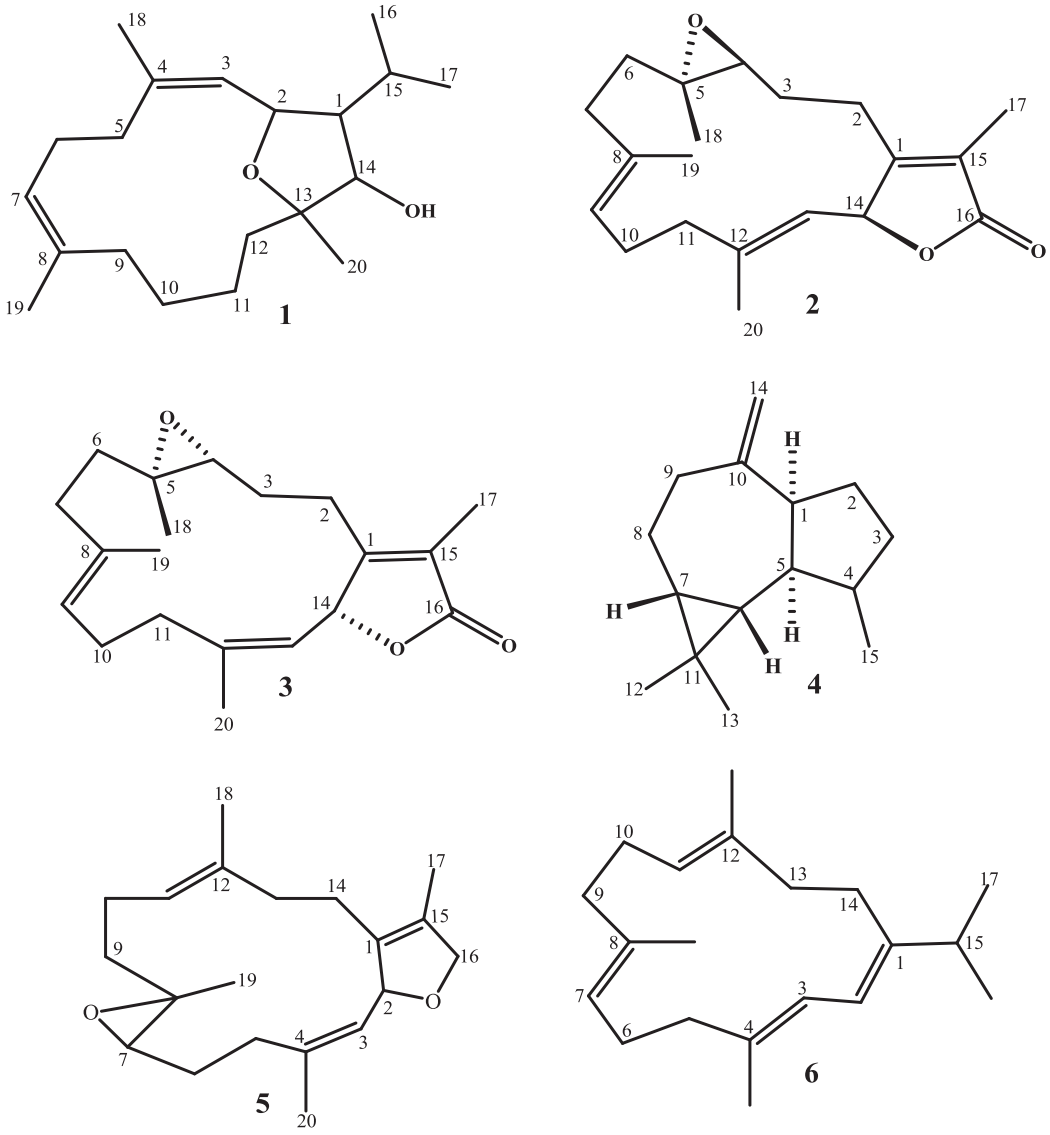

Fig. 1. Compounds isolated from *Sarcophyton glaucum* (**1**–**6**).

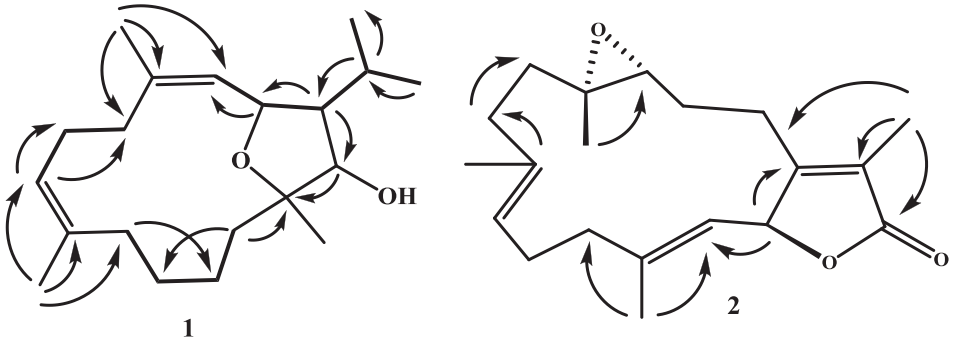

Fig. 2. Selected $^{1}H-^{1}H$ COESY (▬) and HMBC (⟶) correlations of compounds **1** and **2**.

ring, in addition to two carbon–carbon double bonds together with the absence of any other unsaturation imply the existence of one more ring. The nature of the second ring was proved to be 14-membered ring based on the following: a) ^{13}C NMR signals δ_C 125.4 (C-3), 138.6 (C-4), 124.1 (C-7) and 136.0 (C-8) indicated the presence of two non-conjugated trisubstituted double bonds, a deduction supported by absence of characteristic absorption in UV spectrum, b) $^{1}H-^{1}H$ COESY spectral data indicated the possibility to establish three partial structures of consecutive proton systems extending from H_2-5 to H_2-7 through H_2-6; from H_2-9 to H_2-12

Table 2
^{1}H [$CDCl_3$, 600 MHz] and ^{13}C NMR [$CDCl_3$, 150 MHz] NMR spectral data of **5**–**6**.[a]

P.	**5**		**6**	
	δ_C[c]	δ_H[b]	δ_C	δ_H
1	128.0	–	147.0	–
2	83.7	5.54 (brd, 9.0 Hz)	118.5	6.06 (d, 10.8 Hz)
3	126.3	5.23 (d, 9.0 Hz)	121.9	5.99 (dd, 10.8, 1.2 Hz)
4	139.5	–	134.7	–
5	38.0	2.33–2.35 (m)	38.9	2.13–2.15 (m)
6	25.3	1.89–1.91 (m) 1.61–1.63 (m)	25.3	2.20–2.21 (m)
7	62.0	2.7 (t, 7.2 Hz)	125.0	5.03–5.05 (m)
8	60.0	–	134.5	–
9	39.9	2.08–2.10 (m) 1.08–1.10 (m)	38.6	2.15–2.17 (m)
10	23.5	2.23–2.25 (m) 1.89–1.91 (m)	38.6	2.13–2.15 (m)
11	123.6	5.10 (dd, 6.0, 4.8 Hz)	124.5	5.02–5.03 (m)
12	136.8	–	134.7	–
13	36.9	1.90–1.92 (m)	39.1	2.10–2.12 (m)
14	26.1	2.53–2.55 (m) 1.65–1.66 (m)	28.0	2.34–2.36 (m)
15	131.4	–	33.8	2.33–2.35 (m)
16	78.3	4.49–4.51 (m)	22.3	1.09 (d, 6.6 Hz)
17	10.2	1.65 (s)	22.3	1.09 (d, 6.6 Hz)
18	15.1	1.61 (s)	17.1	1.63 (s)
19	16.9	1.27 (s)	15.6	1.55 (d, 4.2 Hz)
20	15.6	1.83 (br s)	17.0	1.78 (br s)

[a] All assignments are based on 1D and 2D measurements (HMBC, HSQC, COESY).
[b] Implied multiplicities were determined by DEPT (C = s, CH = d, CH_2 = t).
[c] *J* in Hz.

through H_2-10 and H_2-11, and finally from H-1 to H-3 through H-2, c) the connectivities of these partial structures were further established by interpretation of the HMBC correlations (Fig. 2) between the carbons of the three parts as observed from H_3-16 to C-15, C-17, C-1, C-2, C-3, C-4; from H_3-18 to C-3, C-4, C-5, C-6, C-7, and C-8; From H_3-19 to C-8, C-9, C-10, C-11, C-12, C-13, and C-14. Hence, metabolite **1** represents the typical cembranoid-like structure which fitted with the published data [8–12].

The relative configuration of **1** assigned by 2D NOESY spectral data, which indicated the presence of cross peaks between the vinylic CH_3-18 and H_2-6, suggested the *E* geometry for the C-3/C-4 double bond, which was also identified by the chemical shift of H-3 at δ_H 5.25. The geometry of the trisubstituted olefin at C-3/C-4 is *E* oriented owing to the values of chemical shifts of allylic methylene $\delta_C > 30$ and the *J* values. Cross peaks were assigned between the vinylic CH_3-19 and H_2-6 suggested the *E* geometry for the C-7/C-8 double bond, which was also identified by the chemical shift of H-7 at δ_H 5.00. The geometry of the trisubstituted olefin at C-7/C-8 was assigned as *E* based on the higher field chemical shift of the olefinic methyl signal for C-19. Furthermore, the NOE correlations between H-2/H-1, Me-18/H-1, Me-19/H_2-10, Me-20/H-3, Me-18/Me-16, and Me-18/H_2-12, demonstrated the 2*S**, 7*S**, and 8*S** configurations as depicted in Fig. 2. A careful analysis of all the NMR spectroscopic data (COESY, HSQC, HMBC, and NOESY) confirmed (**1**) to be cembranoid derivatives. A computer survey was done employing science finder indicated compound **1** is new natural metabolite. For **1**, a trivial name sarcophytolol was given.

Table 3
Cytotoxic activity of the compounds **1**–**4**, against selected cancer cell lines.

Comp. No.	IC_{50} (μM)[a,b]			
	HepG2	MCF-7	A549	PC-3
Total extract	4.6 ± 0.012	53.1 ± 0.123	35.8 ± 0.034	17.3 ± 0.154
1	20.0 ± 0.032	NA	196.7 ± 0.032	31.5 ± 0.053
2	94.0 ± 0.022	25.0 ± 0.160	73.8 ± 0.042	216.5 ± 0.164
3	20.0 ± 0.153	29.0 ± 0.030	200.7 ± 0.164	112.4 ± 0.032
4	20.0 ± 0.068	20.0 ± 0.054	98.4 ± 0.120	09.3 ± 0.164
Doxorubicin	0.48 ± 0.022	0.64 ± 0.038	0.22 ± 0.012	0.50 ± 0.014

Human hepatocellular liver carcinoma (HepG2), human breast adenocarcinoma (MCF-7), Lung carcinoma (A549) and Prostate cancer (PC-3).
Data are presented as mean ± standard deviation, SD.
NT: non toxic at concentrations >100 μM.
[a] IC_{50} of the total extract is expressed as μg/mL.
[b] All compounds showed no cytotoxic effect at >100 μM on normal adult African green monkey kidney (VERO).

Compound **2** was isolated as colorless oil (10.0 mg) with $[\alpha]_D^{22}$ – 90.0 (c 0.02, $CHCl_3$). The LCESIMS (Negative-ion-mode) of **2**, exhibited *m/z* 315.18 $[M - H]^+$, consistent with molecular formula $C_{20}H_{28}O_3$ (seven unsaturations) and validated by HRESIMS (Positive-ion-mode) *m/z* 317.2118 $[M + H]^+$, calculated for $C_{20}H_{28}O_3$ *m/z* 316.2038. The IR spectrum indicated the presence of an α, β-unsaturated-γ-lactone (υ_{max} 1750 cm^{-1}), an olefin (1669 cm^{-1}), and an epoxide (1256 cm^{-1}) functionalities. ^{13}C (^{1}H decoupled) and DEPT NMR experiments (Table 1) exhibited 20 carbon signals establishing: four methyles, six methylenes, four methines (two are oxygenated), six quaternary carbons, one of which is a carbonyl carbon.

Careful examination of the ^{13}C NMR spectral data revealed clear evidences for the presence of trisubstituted epoxy ring resonating at δ_C 61.4 (C-4, d) and 59.9 (C-5, s) assigned for C-4 and C-5, respectively; an α, β-unsaturated-γ-lactone based on characteristic signals resonating at δ_C 174.0 (C-16, s), 120.6 (C-15, s) and 162.2 ppm (C-1, s); two trisubstituted C=C bonds resonating at δ_C 124.9 (C-9, d), 144.1 (C-8, s), 135.6 (C-12, s) and 121.0 ppm (C-13, d) and finally, an oxymethine carbon which appeared at δ_C 78.8 ppm (C-14, d).

^{1}H NMR spectral data indicated the presence of three olefinic methyl protons resonating at δ_H 1.65, 1.91 and 1.88; a paraffinic methyl protons resonating at 1.28; two oxymethine protons at δ_H 2.68 and at δ_H 5.57 and two olefinic protons at δ_H 5.17 ppm (dd, 9.6, 5.4 Hz; H-9) and δ_H 5.05 ppm (dd, 10.2, 1.2 Hz; H-13).

^{1}H–^{1}H COESY spectral interpretation showed the correlation between the methine proton signal resonating at δ_H 2.68 (H-4) and the CH_2 protons at 1.90 and 1.70 ppm (H-3) and CH_2 protons at δ_H 2.40 ppm (H-2) established the connectivity of the H-2/H-3/H-4 (Fig. 2). The second sequence was established from the correlations between the methine protons resonating at δ_H 5.17 (H-9) and the CH_2 protons at δ_H 2.13 ppm (H-7), which in turn are correlated to signal of CH_2 protons at δ_H 1.10 (H-6) confirm the connectivity of the H-6/H-7/H-8. Further investigation of the ^{1}H–^{1}H COESY indicated the correlations of CH_2 protons resonated at δ_H 2.40 (H-10) with the CH_2 protons at δ_H 2.10 (H-11) and δ_H 2.78 ppm (H-11) led to the connectivity of the H-10/H-11. Finally, an oxymethine proton H-14 in correlation with an olefinic proton H-13, led to the connectivity of the H-13/H-14.

The HMBC correlations between the methyl protons H_3-17 with C-1, C-15 and C-16; correlation between oxymethine proton H-14 with C-2 and C-13 led to establishing a trisubstituted furenone moiety. The methyl protons signal resonating at δ_H 1.28 (s, H_3-18) indicated a proximal oxygen functionality identified from ^{13}C NMR to be an epoxide (Table 1).

The location of the epoxide ring at C4/C-5 was detected from HMBC correlations (Fig. 2), as there are clear correlations between H-4 with C-2, C-3 and C-5, also correlation between H_3-18 with C-4, C-5 and C-6, and between H_2-3 and C-1 established the connections from C-1 to C-6. The olefinic methyl protons at δ_H 1.91 ppm (H_3-19), also show an HMBC correlation with C-7, C-8 and C-9, while the olefinic proton H-9 is correlated to C-7 and C-8, led to establishing the connections from C-7 to C-10. Remaining is the connections from C-11 to C-14 were deduced from the HMBC correlations between the olefinic methyl protons H_3-20 with C-11, C-12 and C-13.

An extensive computer survey about soft corals indicated that Sarcophyton is the factory of cembranoids. Deep investigation of these literatural data [13–19], and comparing it with the obtained data, indicated that **2** has C-14 cembrane skeleton. The molecular framework containing position of the epoxide moiety is shifted to be C-4/C-5. The vicinal coupling constant of 10.2 Hz between H-13 and H-14 as well as 2D NMR NOESY correlation of H-14 with H_3-20 established an *E*-configuration between the γ-lactone (H-14) and the olefinic proton (H-13). Further investigation of 2D NOESY spectral data indicated the absence of correlation between CH_3-18 and H-4 indicated the methyl group has β-configuration and the oxiran junction will be identified as 5R* and 4S* (Fig. 1). Also NOSEY correlations between H-11 and H-13; between H-9 and H-10; between H_3–H-4 and H-9, led to *E*-configuration of the C=C double bond between C-12 and C-13. A computer survey was done employing science finder indicated **2** is new cembranoid derivative. For **2**, a trivial name sarcophytolide B is given.

Compound **3** was obtained as colorless oil (9.0 mg) with $[\alpha]_D^{22}$ − 60.0 (c 0.015, $CHCl_3$). The negative mode of LCMS exhibited a $[M - H]^+$ *m/z* 315.180, indicating a molecular formula of $C_{20}H_{28}O_3$ and validated by HRESIMS (Positive-ion-mode) *m/z* 317.2110 $[M + H]^+$. The seven degrees of unsaturation were supported by NMR data. The IR spectrum indicated the presence of α, β-unsaturated-γ-lactone (1750 cm^{-1}), an olefin (1669 cm^{-1}), and an epoxide (1256 cm^{-1}) functions. The ^1H and ^{13}C NMR spectral data of **3** are closely similar to that of **2**, although during separation process they are quietly differed in the retention factor (R_f), which tempted us to check the difference in stereochemistry between **2** and **3**. 2D NOESY NMR spectral data was employed for assigning of the relative configuration of **3** (Fig. 2). The presence of a NOESY cross peak between the vinylic H-9 and H-10, cross peaks between CH_3-20 and H-10, indicated the *Z* geometry of both C-8/C-9 and *Z* geometry C-12/C-13 double bonds. This deduction supported by the chemical shift of H-14 at δ_H 4.99.

Furthermore, the conclusive NOE correlations between H-14 and H-1; between H-14 and CH_3-20; between H-3 and H_3-18, confirmed the *Z* geometry of the two vinylic double bonds. The presence of cross peaks between CH_3-18 and H-4 indicate the oxiran junction will be identified as 5R* and 4R* configuration (Fig. 1). After survey employing different data bases includes science finder, indicates **3** is new natural cembranoid derivative. For **3**, a trivial name sarcophytolide C is given.

Compounds (**4**–**6**) were identified by comparison the measured spectral data with the published [20–24] (Table 2).

2.2. Biology

Compounds **1**–**4** were evaluated to assess their Antiproliferative effect towards five different cell lines (MCF-7, HepG2, A549, PC-3 and VERO) in comparison to standard anticancer drug (Doxorubicin), by employing MTT assay. The tested compounds showed considerable antiproliferative activity selectively against different three cancer cell lines. Wealthy that **1** and **4** showed significant activities to HepG2 (IC_{50} 20 ± 0.032 and 20 ± 0.068 μM, respectively) and to PC-3 (IC_{50} 31.5 ± 0.053 and 9.3 ± 0.164 μM, respectively). Compounds **2** and **3** showed activity to MCF-7 (IC_{50} 25 ± 0.0164 and 29 ± 0.030 μM, respectively), while **3** showed potent activity to HepG2 (IC_{50} 20 ± 0.153 μM). The antiproliferative activity of **1**, **3** and **4**, was attributed to effects G0/G1 and S-phase cell cycle arrest.

On the other hand, the IC_{50} of the tested compounds (**1**–**4**) in A549 cell lines was significantly higher (IC_{50} ranges from 98.4 ± 0.12 to 196.7 ± 0.032 μM) and less potent compared to MCF-7 and HepG2 cells. **4** had potent antiproliferative effect towards PC-3 with IC_{50} 9.3 ± 0.164 μM. Finally, no cytotoxicity of all metabolites was observed with VERO cells even at 100 μM.

It is wealthy to study the mechanism of action of the significant cytotoxic activities. Thus, the cell cycle analysis for the potent and the available metabolites (**1**, **3** and **4**) drugs were processed. **1** and **3** were evaluated to their effects on cancer cell cycle phases of HepG2 and **4** was evaluated to on cell cycle of PC-3 comparing with untreated cells (Fig. 3A). **1** and **3** decreased cell population in S-phase from 43.65 ± 1.1% (Fig. 3A) to 8.33 ± 0.9% (Fig. 3B) and 7.11 ± 0.5% (Fig. 3C), respectively, were obtained. Both **1** and **3** induced compensatory increase in the non-proliferating cell fraction (G0/G1-phase) from 44.74 ± 0.6% (Fig. 3A) to 53.57 ± 0.7% (Fig. 3B) and 51.90 ± 0.2% (Fig. 3C), respectively.

DNA flow-cytometry of **4** was performed in PC-3 cell lines compared to untreated cells (Fig. 3). **4** decreased cell population in S-phase from 32.12 ± 0.9% (Fig. 3D) to 23.29 ± 0.9% (Fig. 3E) and induced compensatory increase in the non-proliferating cell fraction (G_0/G_1-phase) from 49.80 ± 0.6% (Fig. 3D) to 64.83 ± 0.7% (Fig. 3E).

Subsequent to the decrease in S-phase, **4** induced considerable decrease in G_2/M-phase. The influence of **4** on cell cycle progression of PC-3 cells was 08.83 ± 0.3% to S-phase cell population which increased in the non-proliferating cell fraction (G0/G1-phase) by 15.05 ± 0.3%. From these results, it can be conclude that the cembranoids which isolated in this study were attributed to effects G0/G1 and S-phase cell cycle arrest.

To further substantiate the potential apoptotic activity of compounds **1**, **3** and **4**, caspase-3 concentration was assessed in the responsive cell lines. Exposure of HepG2 cells to **1** and **3** significantly caused 2.6 and 2.0-folds increase in the concentration of caspase-3 respectively, as compared to untreated cells (Fig. 4). In addition, **4** caused a 2.1-fold increase in the concentration of caspase-3 in PC-3 compared to untreated cells (Fig. 4). These data gain support by the observed ability of the compounds to cause accumulation of cells in the pre-G phase of cell cycle. These data gained further support by assessing the proportion of cells stained by annexin V; which give accurate indication of both early and late apoptosis as shown in Fig. 5. The Flow Cytometric Analysis revealed that HepG2 cells treated with compounds **1** and **3** showed a significant increase in the percent of annexin V–FITC-positive apoptotic cells (UR, Late apoptotic + LR, Early apoptotic) when compared to untreated HepG2 cells. Exposure of PC-3 cells to compound **4** resulted in a significant elevation in annexin V–FITC-positive apoptotic cells (UR + LR) by more than 10 folds that of the untreated cells.

Therefore, it can be concluded that induction of apoptosis, at least partly, mediate the antiproliferative activity of sarcophytolol (**1**), sarcophytolide C (**3**) and 10(14) aromadendrene (**4**).

3. Experimental

3.1. General

Optical rotations were measured on ATAGO POLAX-L 2 polarimeter. EI/MS analyses were carried out on a Shimadzu-QP 2010. GC/MS analyses were carried out usigRTX-1 column (30 m, 0.25 mm) was used. 1D and 2D NMR spectra were recorded on Bruker AVANCE III WM 600 MHz spectrometers and ^{13}C NMR at 150 MHz. Chemical shift values are given in δ(ppm) relative to TMS as internal standard. Thin layer chromatography was performed on silica gel (Kieselgel 60, F_{254}) of 0.25 mm layer thickness. Gel filtration was carried out using Sephadex LH-20. Spots were detected by using ethanol/sulfuric acid as spray reagent.

3.2. Animal material

Soft coral *S. glaucum* (Order Alcyonacea, Family Alcyoniidae) was collected from the North of Jeddah Saudi Arabia Red Sea coast

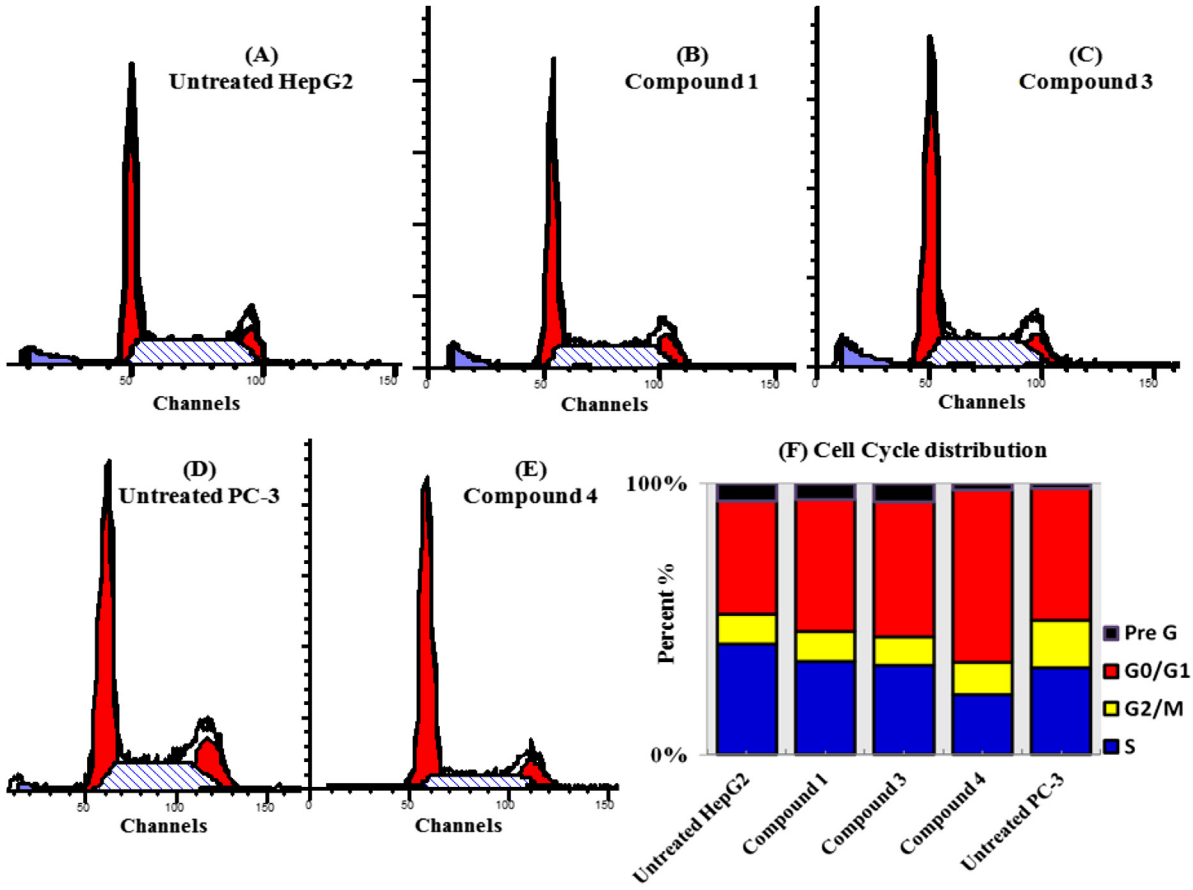

Fig. 3. Effect of **1** and **3** on the cell cycle distribution of HepG2 and **4** on the cell cycle distribution of PC-3. HepG2 cancer cells were exposed to **1** (B), **3** (C) for 24 h and compared to untreated cells (A). PC-3 cancer cells were exposed to **4** (E) for 24 h and compared to untreated cells (D). Cell cycle distribution was determined using DNA cytometry analysis and different cell phases (F) were plotted as percent of total events ($n = 3$).

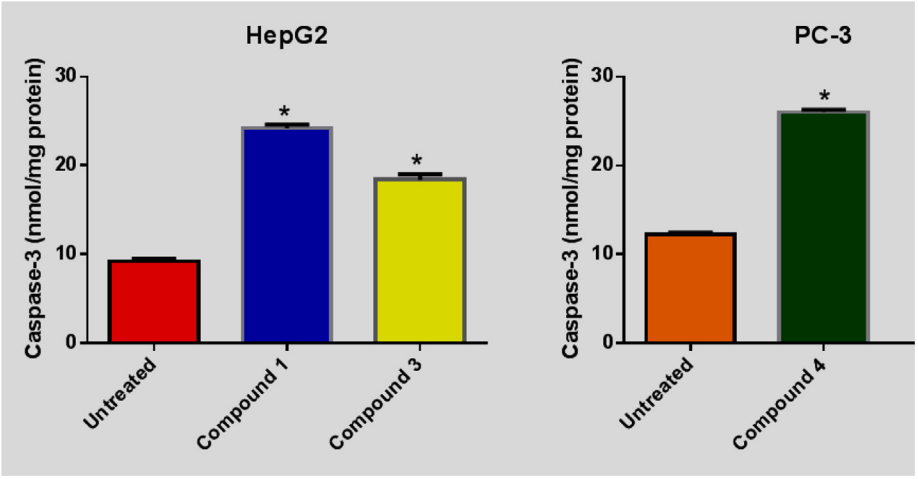

Fig. 4. Effect of compounds **1**, **3** and **4** on caspase-3 activity in selected cancer cells lines. Differences between compound **4** and corresponding control value were checked using unpaired Student's *t* test. *Significantly different from corresponding untreated control at $p < 0.05$.

(21°29′31″N 39°11′24″E) in Jeddah, at a depth of 5 m, in May, 2012. After collection of this material was immediately subjected to the extraction. A voucher specimen (SC-2012-8) was deposited in the faculty of Marine Science, King Abdulaziz University, Jeddah, Saudi Arabia.

3.3. Extraction and isolation

The fresh Soft coral *S. glaucum* (3.0 kg) was minced and extracted by diethyl ether at room temperature (22 °C, 3 × 5 L), yielded viscous blackish residue (20 g), was fractionated on NP-

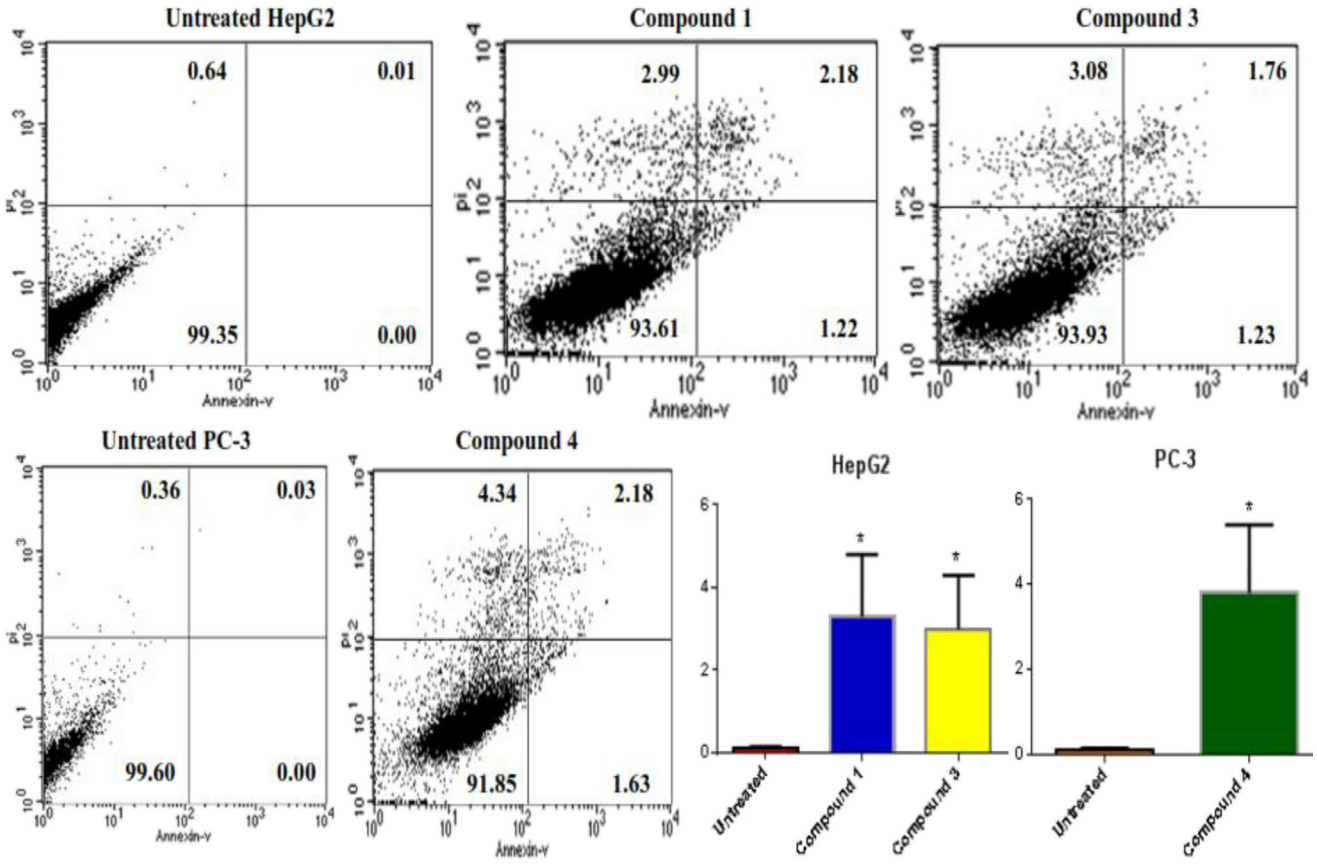

Fig. 5. Effects of compounds **1**, **3** and **4** on the percentage of responsive cells (HepG2 or PC-3) on annexin V–FITC-positive staining. Data represent mean ± SD. The four quadrants identified as LL (viable); LR (early apoptotic); UR (late apoptotic) and UL (necrotic). *Significantly different from corresponding untreated control at $p < 0.05$.

Silica employing gradient elution from *n*-hexane to EtOAc, followed by dichloromethane to acetone ($\Phi = 50$, $L = 100$ cm, 100 mL each), 20 fractions were collected. The fractions were investigated by ^{1}H NMR and TLC pattern using UV lamp and/or 50%-sulfuric acid in methanol as spraying reagent. All compounds were purified by PTLC and re-purified by employing Sephadex LH-20 ($\Phi = 5$, $L = 10$ cm, 5 mL each) using a mixture of MeOH:$CHCl_3$ (9:1). Fraction 3 was purified by RP-18 HPLC (MeOH/H_2O, 75:25) to afford **4** (15 mg, 0.005%). Fraction 5 was purified by was purified by RP-18 HPLC (MeOH/H O, 85:15) to afford yielded **1** (8.0 mg, 0.0026%) and **2** (9.0 mg, 0.003%). Fraction 8 was purified by RP-18 HPLC (MeOH/H O, 65:35) yielded **3** (10 mg, 0.0033%).

3.3.1. Sarcophytolol (*1*)

Colorless oil (8.0 mg, 0.0084%); $[\alpha]_D^{22} + 10.0$ (*c* 0.02, $CHCl_3$); IR λ_{max} (film) cm^{-1}: 3713 (O–H), 3423 (O–H), 2937 (C–H), 1645 (C=C), 1378, 1221, 1045; ^{13}C NMR ($CDCl_3$, 150 MHz) and ^{1}H NMR ($CDCl_3$, 600 MHz) spectroscopic data (Table 1); HRESIMS (positive mode) $m/z = 307.2637$ $[M + H]^+$ (Calculated $m/z = 306.2559$ for $C_{20}H_{34}O_2$).

3.3.2. Sarcophytolide B (*2*)

Colorless oil (10.0 mg); $[\alpha]_D^{22} - 90.0$ (c 0.02, $CHCl_3$); IR λ_{max} (film) cm^{-1}: 3472 (O–H), 2925 (C–H), 1748 (C=O), 1654 (C=C), 1392, 1090, 771; ^{13}C NMR ($CDCl_3$, 150 MHz) and ^{1}H NMR ($CDCl_3$, 600 MHz) spectroscopic data, (Table 1); HRESIMS (Positive-ion-mode) *m/z* 317.2118 $[M + H]^+$ (Calculated $m/z = 316.2380$ for $C_{20}H_{28}O_3$).

3.3.3. Sarcophytolide C (*3*)

Colorless oil (9.0 mg); $[\alpha]_D^{22} - 60.0$ (c 0.015, $CHCl_3$); IR λ_{max} (film) cm^{-1}: 3472 (O–H), 2925 (C–H), 1748 (C=O), 1650 (C=C), 1388, 1086, 763; ^{13}C NMR ($CDCl_3$, 150 MHz) and ^{1}H NMR ($CDCl_3$, 600 MHz) spectroscopic data (Table 1); HRESIMS (Positive-ion-mode) *m/z* 317.2110 $[M + H]^+$ (Calculated $m/z = 316.2380$ for $C_{20}H_{28}O_3$).

3.4. Biological evaluation

3.4.1. Antiproliferative bioassays

Compounds **1**–**4** were tested against five cancer cell lines; Human hepatocellular liver carcinoma (HepG2), human breast adenocarcinoma (MCF-7), Lung carcinoma (A549), Prostate cancer (PC-3) and normal adult African green monkey kidney (VERO). The percentage of viability of cell was estimated by using doxorubicin as a positive standard anticancer drug. These assays had been performed according to the published protocols [13]. The stock samples were diluted with RPMI-1640 Medium to desired concentrations ranging from 10 to 1000 μg/mL. The final concentration of dimethylsulphoxide (DMSO) in each sample did not exceed 1% v/v. The cancer cells were batch cultured for 10 d, then seeded in 96 well plates of 10×10^3 cells/well in fresh complete growth medium in 96-well Microtiter plastic plates at 37 °C for 24 h under 5% CO_2 using a water jacketed carbon dioxide incubator (Shedon.TC2323.Cornelius, OR, USA). The medium (without serum) was added and cells were incubated either alone (negative control) or with different concentrations of sample to give a final concentrations of (1000, 500, 200, 100, 50, 20, 10 μg/mL). Cells were suspended in RPMI-1640 medium, 1% antibiotic–antimycotic mixture (10^4 μg/mL potassium penicillin, 10^4 μg/mL streptomycin sulfate and 25 μg/mL Amphotericin (B)) and 1% L-glutamine in 96-well flat bottom micro-plates at 37 °C under 5% CO_2. After 96 h of

incubation, the medium was again aspirated, trays were inverted onto a pad of paper towels, the remaining cells rinsed carefully with medium, and fixed with 3.7% (v/v) formaldehyde in saline for at least 20 min. The fixed cells were rinsed with water, and examined. The cytotoxic activity was identified as confluent, relatively unaltered mono-layers of stained cells treated with compounds. The IC_{50} was calculated based on the 50% loss of monolayer and 5-Fluorouracil was used as a positive control. To calculate IC_{50}, a series of dose–response data (e.g., drug concentrations $x1$, $x2$, …, xn and growth inhibition $y1$, $y2$, …,yn), were plotted and the values of y are in the range of 0–1. The simplest estimate of IC_{50} is to plot X–Y and fit the data with a straight line.

3.4.2. Analysis of cell cycle distribution

To assess the effect of the test compounds on cell cycle distribution, cells were treated with the pre-determined IC_{50} of test compounds for 24 h and collected by trypsinization, washed with ice-cold PBS, and re-suspended in 0.5 mL of PBS [13]. 10 mL of 70% ice-cold ethanol was added gently while vortexing and cells were kept at 4 °C for 1 h and stored at −20 °C until analysis. Upon analysis, fixed cells were washed and re-suspended in 1 mL of PBS containing 50 μg/mL RNase A and 10 μg/mL propidium iodide (PI). After 20 min incubation at 37 °C, cells were analyzed for DNA contents by FACSVantageTM (Becton Dickinson Immunocytometry Systems, San Jose, CA). For each sample, 10,000 events were acquired. Cell cycle distribution was calculated using CELLQuest software (Becton Dickinson Immunocytometry Systems, San Jose, CA). Cells treated with doxorubicin were used as positive control sample.

3.4.3. Caspase-3 concentration assay

Caspase-3 was assessed by colorimetric assay kit (Cloud-Clone Corp., Houston, TX). Approximately, 2×10^6 cells were harvested and the pellet was suspended in lysis buffer. Protein levels were determined by Bradford assay (Bio-Rad Laboratories, Hercules, CA). Aliquots of 100 μL of cell lysate (total protein, approximately 100 mg) were incubated with detection reagents and then with 90 μL of substrate at 37 °C for 25 min as indicated by the manufacturer. Developed color was measured at 450 nm using microplate reader (ChroMate-4300, Palm City, FL). Caspase-3 concentration was expressed as nmol/mg protein.

3.4.4. Annexin V. Assay

Annexin V–FITC Apoptosis Assay of the responsive cells (HepG2 and PC-3) were seeded as described above and then incubated with different treatments for 24 h. Cells were harvested, washed twice with PBS and centrifuged. In brief, 1×10^5 of cells were treated with annexin V–FITC and propidium iodide (PI) using the apoptosis detection kit (BD Biosciences, San Jose, CA) according to the manufacturer's protocol. Annexin V–FITC and PI binding were analyzed by flow cytometry on FACScalibur (BD Biosciences, San Jose, CA) without gating restrictions using 10,000 cells. Data were collected using logarithmic amplification of both the FL1 (FITC) and the FL2 (PI) channels. Quadrant analysis of co-ordinate dot plots was performed with CellQuest software. Unstained cells were used to adjust the photomultiplier voltage and for compensation setting adjustment to eliminate spectral overlap between the FL1 and the FL2 signals.

3.4.5. Statistical analysis

Data are presented as mean ± SD. Unless otherwise indicated, comparisons were carried out using one-way analysis of variance followed by Tukey–Kramer's test for post hoc analysis. Statistical significance was acceptable to a level of $p < 0.05$. All statistical analyses were performed using GraphPad InStat software, version 3.05 (GraphPad Software, La Jolla, CA). Graphs were plotted using GraphPad Prism software, version 6.00 (GraphPad Software, La Jolla, CA).

Conflict of interest

All authors declare that there is no conflict of interest.

Acknowledgments

This project was funded by the Deanship of Scientific Research (DSR), King Abdulaziz University, Jeddah, under Grant No. 411/150/1433. The authors, therefore, acknowledge with thanks DSR for technical and financial support. Dr. Yahia, Folos, Researcher, Marine Biology department, Faculty of marine Sciences, King Abdulaziz University, is acknowledged for collection and identification of the soft coral sample.

Appendix A. Supplementary data

Supplementary data related to this article can be found at http://dx.doi.org/10.1016/j.ejmech.2014.05.016.

References

[1] J.G. Burgess, New and emerging analytical techniques for marine biotechnology, Curr. Opin. Biotechnol. 23 (2012) 29–33.
[2] B. Haefner, Drugs from the deep: marine natural products as drug candidates, Drug Discov. Today 15 (2003) 536–544.
[3] A.J. Edwards, S.M. Head, Key Environments-Red Sea, Pergamon Press, Oxford, UK, 1987, p. 440.
[4] P.A. Roethle, D. Trauner, The chemistry of marine furanocembranoids, pseudopteranes, gersolanes, and related natural products, Nat. Prod. Rep. 25 (2008) 298–317.
[5] J. Rocha, L. Peixe, N.C.M. Gomes, R. Calado, Cnidarians as a source of new marine bioactive compounds; an overview of the last decade and future steps for bioprospecting, Mar. Drugs 9 (2011) 1860–1886.
[6] I. Wahlberg, A.M. Eklund, Cembranoids, pseudopteranoids, and cubitanoids of natural occurrence, Prog. Chem. Org. Nat. 59 (1992) 141–294.
[7] S.-Y. Cheng, S.-K. Wang, S.-F. Chiou, C.-H. Hsu, C.-F. Dai, M.Y. Chiang, C.-Y. Duh, Cembranoids from the octocoral *Sarcophyton ehrenbergi*, J. Nat. Prod. 73 (2010) 197–203.
[8] Y.-B. Cheng, Y.-C. Shen, Y.-H. Kuo, A.T. Khalil, Cembrane diterpenoids from the taiwanese soft coral *Sarcophyton stolidotum*, J. Nat. Prod. 71 (2008) 1141–1145.
[9] R. Duffy, C. Wade, Discovery of anticancer drugs from antimalarial natural products: a Medline literature review, Drug Discov. Today 17 (2012) 942–953.
[10] M.-E.F. Hegazy, A.M. Gamal Eldeen, A.A. Shahat, F.F. Abdel-Latif, T.A. Mohamed, B.R. Whittlesey, P.W. Paré, Bioactive hydroperoxyl cembranoids from the Red Sea soft coral *Sarcophyton glaucum*, Mar. Drugs 10 (2012) 209–222.
[11] X. Zhifang, W. Bie, W. Chen, D. Liu, L. van Ofwegen, P. Proksch, W. Lin, Sarcophyolides B–E, new cembranoids from the soft coral *Sarcophyton elegans*, Mar. Drugs 11 (2013) 3186–3196.
[12] S.-K. Wang, M.-K. Hsieh, C.-Y. Duh, New diterpenoids from soft coral *Sarcophyton ehrenbergi*, Mar. Drugs 11 (2013) 4318–4327.
[13] W.M. Alarif, A. Abdel-Lateff, A.M. Al-Abd, S.A. Basaif, F.A. Badria, M. Shams, S.-E. Ayyad, Selective cytotoxic effects on human breast carcinoma of new methoxylated flavonoids from *Euryops arabicus* grown in Saudi Arabia, Eur. J. Med. Chem. 66 (2013) 204–210.
[14] G.-H. Wang, H.-C. Huang, J.-H. Su, C.-Y. Huang, C.-H. Hsu, Y.-H. Kuo, J.-H. Sheu, Crassocolides N-P, three cembranoids from the Formosan soft coral *Sarcophyton crassocaule*, Bioorg. Med. Chem. Lett. 21 (2011) 7201–7204.
[15] J.-H. Su, A.F. Ahmed, P.-J. Sung, C.-H. Chao, Y.-H. Kuo, J.-H. Sheu, Manaarenolides A–I, diterpenoids from the soft coral *Sinularia manaarensis*, J. Nat. Prod. 69 (2006) 1134–1139.
[16] Y. Lu, C.-Y. Huang, Y.-F. Lin, Z.-H. Wen, J.-H. Su, Y.-H. Kuo, M.Y. Chiang, J.-H. Sheu, Anti-inflammatory cembranoids from the soft corals *Sinularia querciformis* and *Sinularia granosa*, J. Nat. Prod. 71 (2008) 1754–1759.
[17] S.-K. Wang, M.-K. Hsieh, C.-Y. Duh, Three new cembranoids from the Taiwanese soft coral *Sarcophyton ehrenbergi*, Mar. Drugs 10 (2012) 1433–1444.
[18] B.-W. Chen, C.-H. Chao, J.-H. Su, C.-Y. Huang, C.-F. Dai, Z.-H. Wen, J.-H. Sheu, A novel symmetric sulfur-containing biscembranoid from the Formosan soft coral *Sinularia flexibilis*, Tetrahedron Lett. 44 (2010) 5764–5766.

[19] J.W. Blunt, B.R. Copp, W.P. Hu, M.H.G. Munro, P.T. Northcote, M.R. Prinsep, Marine natural products, Nat. Prod. Rep. 25 (2008) 35–94.
[20] H.-C. Huang, C.-H. Chao, Y.-H. Kuo, J.-H. Sheu, Crassocolides G-M, cembranoids from the Formosan soft coral *Sarcophyton crassocaule*, Chem. Biodivers. 6 (2009) 1232–1242.
[21] H.-C. Huang, A.F. Ahmed, J.-H. Su, Y.-C. Wu, M.Y. Chiang, J.-H. Sheu, Crassolides A-F, cembranoids with a trans-fused lactone from the soft coral *Sarcophyton crassocaule*, J. Nat. Prod. 69 (2006) 1554–1559.
[22] S.Y. Cheng, C.T. Chuang, Z.H. Wen, S.K. Wang, S.F. Chiou, C.H. Hsu, C.F. Dai, C.Y. Duh, Bioactive norditerpenoids from the soft coral *Sinularia gyrosa*, Bioorg. Med. Chem. 18 (2010) 3379–3386.
[23] Y. Lu, J.H. Su, C.Y. Huang, Y.C. Liu, Y.H. Kuo, Z.H. Wen, C.H. Hsu, J.H. Sheu, Cembranoids from the soft corals *Sinularia granosa* and *Sinularia querciformis*, Chem. Pharm. Bull. 58 (2010) 464–466.
[24] U. Warmers, W.A. König, Sesquiterpene constituents of the liverwort *Calypogeia fissa*, Phytochemistry 52 (1999) 695–704.